Desalination and Water Treatment
www.deswater.com

doi: 10.5004/dwt.2018.23097

136 (2018) 72–82
December

The performance of a spiral wound RO membrane to desalinate a brackish groundwater in the middle of Iraq

Nagam Obaid Kariem[a], Dawood Eisa Sachit[a,*], Zainab Qader Ismael[a,b]

[a]*Environmental Engineering Department, University of Mustansiriyah, Baghdad 10047, Iraq; emails: dawood.sachit@okstate.edu (D.E. Sachit), nagamob@uomustansiriyah.edu.iq (N.O. Kariem), mafhhm1978@gmail.com (Z.Q. Ismael)*
[b]*Ministry of Environment, Baghdad, Iraq*

Received 6 February 2018; Accepted 9 September 2018

ABSTRACT

In this study, a lab-scale of reverse osmosis (RO) system was used to investigate the performance of a spiral wound RO membrane to desalinate a brackish groundwater of several locations (Mandali, Al-Yusufiya, and Al-Musayyib) in the middle of Iraq. The investigation included different parameters such as permeate conductivity, permeate flux, and membrane salt rejection. In addition, the examinations of this work included studying the influence of feedwater temperature and feedwater pressure on permeate flux and membrane salt rejection. Moreover, foulant analysis by the scanning electron microscope images and the associated energy-dispersive X-ray spectroscopy spectra of the RO membrane after being used for 45 d in an existed pilot plant to treat the groundwater of Mandali location was also performed in this study. The results revealed that the difference in the groundwater quality of the selected locations had a significant effect on the permeate fluxes produced by the RO membrane system. In addition, increasing the feedwater temperature positively influenced the permeate flux and negatively impacted the salt rejection of the RO membrane. Furthermore, foulant analysis exhibited that the foulant accumulated on the RO membrane surface was most likely calcium carbonate ($CaCO_3$) which was apparently in calcite form.

Keywords: Groundwater; Reverse osmosis; Feedwater; Permeate; Fouling; Salt rejection

1. Introduction

The provision and sustainability of potable water are important factors for disease prevention. It can be considered as the foundation of the valid life. Although there are a wide variety of water resources available in the planet, the gap between water supply and demand is getting larger, and it continues to increase due to the worldwide growth in the population and the applications of the water in the commercial and industrial fields which have resulted in more water consumption [1]. Reducing fresh surface water has led to seek other sources such as seawater, brackish groundwater, or treated wastewater as feedwater for the treatment plants to produce drinkable water [2]. Groundwater, which is one of these suitable sources that can be exploited, is mostly saline water and needs to be treated by different techniques to remove salt and other minerals rather than using conventional treatment method [3,4].

One of the most promising methods to desalt saline water is the membrane process [5]. The membrane can be defined as "a physical barrier through which pure solvent can pass while other molecules or particles are retained" [6]. The pressure-driven force membranes can be classified according to the pore size into four types: microfiltration with a nominal pore size range of 1–10 μm, ultrafiltration with a nominal pore size range of 0.01–0.1 μm, nanofiltration with a nominal pore size range of 0.001–0.01 μm, and reverse osmosis (RO) with a nominal pore size range of 0.0001–0.001 μm [7].

* Corresponding author.

In general, the RO membrane process is the well-known separation method used in water desalination technique [8,9]. Several types of materials have been used to make the fabrication of the membrane based on the operating conditions. For example, the synthetic membrane may be classified into organic such as a porous or dense membrane, inorganic such as a ceramic membrane, composite such as that covers both polymeric and inorganic membranes, and nanomaterial–polymeric membranes [10].

Generally, there are three common types of polymers that are used to prepare the RO membranes: cellulose acetate (CA), fully aromatic polyamide (PA), and thin-film composite (TFC) [9–13]. CA membranes are not tolerant to high temperatures and possibly will destroy with high free chlorine concentrations (above 1 mg/L). In addition, they might hydrolyze in low and high pH. CA membranes, however, have a smooth hydrophilic (has affinity for water) surface that makes this type of membrane less susceptible to fouling than the PA membrane which has a rough hydrophobic (has no affinity for water) surface [9,14]. PA membranes, on the other hand, are less susceptible to the biological degradation, and they work more appropriately over a wide range of pH. Furthermore, TFC membranes are made by combining three different layers: thin-film of cross-linked aromatic PA layer (approximately 0.2 microns in thickness), polysulfone layer, and polyester fabric layer. The first layer is the active one which rejects the dissolved and suspended solids of the feedwater while the other two layers are supporting layers. In general, water flux and salt rejection of TFC membranes are higher than those of CA membranes [3,9–12,14,15].

In terms of membrane configuration, four basic modules of RO membranes are typically developed for industrial applications which are plate and frame, tubular, spiral wound, and hollow fine fiber. The most common module of RO membrane that is used in water desalination is the spiral wound configuration which is characterized with high packing density [9,13].

In RO membrane system, a high pressure is applied on the side of the higher solute (salt ion) concentration to force the solvent (water) to pass through a semi-permeable membrane (permeable to the water, but not the salt ions) to the side of the lower solute concentration [16]. The main problem of installing and operating RO membrane system is membrane fouling. Some of other problems are the disposal of waste products and concentrate, trapping of fish or other marine organisms by the screens of the intake structures of the facility, and emission of air pollutants as a result of energy-intensive processes [17,18]. Numerous types of materials may cause RO membrane fouling such as microbial growth (biofilms), organic matters, colloids, particulates, inorganic materials, and suspended particles [9,19]. RO membrane fouling which causes the permeate flux decline by reducing the available area for the solvent to pass through is significantly influenced by several parameters. Solute concentration, for instance, increases the osmotic pressure that enhances concentration polarization and consequently enhances membrane surface fouling [20,21]. Moreover, feedwater temperature has an impact on the morphology of the deposited materials on the surface of the RO membrane. For example, high temperature may enhance the crystal formation of the fouled materials while low temperature may enhance formation of a sludge-like deposit on the RO membrane surface. However, high feedwater temperature causes a reduction in the water viscosity and a swelling in the polymeric membrane, which are resulted in an increase in the permeate flux with higher solute concentration [22,23]. The morphology of the surface of the membrane itself is another factor that has an impact on the accumulation of the fouled materials on the membrane surface. For example, TFC PA RO membrane, as previously mentioned, is more susceptible to fouling than CA RO membrane [22,24].

Brackish water RO membrane performance has been widely studied in order to understand the problems that negatively influence the performance of this technique and to find the solutions to solve or minimize these problems. Because fouling is the main parameter that affects the membrane performance, the main focus in the following literature is on brackish water RO membrane fouling. Fouling develops on RO membrane surface through different layers [25,26]. Each layer has a varied thickness which ranges from less than 1 to about 10 μm [25]. In addition, fouling material is unevenly distributed on the membrane surface [27]. Moreover, fouling of brackish water RO membrane is possible to be controlled under appropriate operating conditions and proper conventional pretreatment to significantly prolong the membrane operating time [26]. Autopsy studies of the RO membranes, which are used to desalinate brackish water, revealed that the predominant compounds in the fouling layer are different and mainly rely on the feedwater quality. For instance, SiO_2, clay, organic matter, $CaSiO_3$, Fe_3O_4, $AlPO_4$, and $CaSO_4$ were the main foulants observed by Karime et al. [28]. However, Yang et al. [29] found that 85%–93% of the total foulants were organic matter in the first stage, while 92%–95% were inorganic matter (mostly calcium) in the second stage. Furthermore, Arras et al. [30] reported that the changes in the quality/quantity of the brackish water can significantly impact the pretreatment unit of the RO system and, consequently affect the deposited material on the membrane surface.

Iraq has various resources of water such as the Tigris and Euphrates rivers, marshes, and plenty of groundwater. However, many regions in Iraq are seriously influenced by the drought conditions in the last decade. In addition, the water level reduction in the Tigris and Euphrates rivers has become more visible because of the low quantity of water that is released from the neighboring countries which manipulated the sources of these two rivers [31]. Other reasons that are resulted in an increase in water demand and have negative impacts on water availability are: population growth, Iraq's location in the semi-arid region, high temperatures and evaporation rates, and human activities such as agricultural, industrial, and urbanization [32]. Therefore, groundwater is sought as an alternative source of water by the people in these regions. Taking advantage of the expansion of the RO membrane process in southern of Iraq to exploit the brackish surface water of the marshes for drinking water purposes [3], this technology started to spread in the middle of Iraq where a real shortage in the fresh surface water is existed. Several pilot desalination plants of RO system relying on the groundwater as a source of the feedwater were implemented in some locations in the middle of Iraq, and more pilot RO plants are expected to be carried out in the future, and therefore,

studies to asses and minimize the problems of operating this technology are required.

Studying the application of the RO system in desalting the groundwater of several locations in the middle of Iraq was presented in this work. This examination included the effect of the variability of the groundwater quality of three selected locations on the permeate fluxes produced by the RO membrane system. In addition, the influence of the operating conditions such as feedwater temperature and feedwater pressure on membrane performance was also investigated. Moreover, to observe the main foulants and the scale formation on the RO membrane surface, an autopsy analysis by the scanning electron microscope (SEM) images and the associated energy-dispersive X-ray spectroscopy (EDXS) spectra of used RO membrane was also performed in this study. The selected RO membrane for the autopsy analysis was in operation for 45 d in an existed pilot plant to treat the groundwater of Mandali location.

2. Material and methods

2.1. Feedwater

Several different sources of groundwater located in the middle of Iraq were used to evaluate using RO membrane system in producing drinkable water. These sources were considered as an alternative to the fresh surface water which is significantly reduced in these three selected places in the last two decades. The first place that was considered in this study is Mandali which is a town in the Balad Ruz District, Diyala province, near the Iran–Iraq border as shown in Fig. 1. The population of Mandali in 2014 was 120,000 capita. Kinkar River was the main source of freshwater for this town. However, when a dam was built on this river in the Iranian side in the mid of the last century and caused the river valley to dry out, the quantity and the good quality of the freshwater have become limited to this region. Therefore, several pilot RO plants were established in this region, relying on groundwater as a source of the feedwater. To study the performance of the RO system in this area, samples of 200 L of groundwater were taken from two wells which have a total dissolved solids (TDS) range of 1,300–1,400 mg/L. Water analyses were performed for these two samples and the results of the main parameters are illustrated in Table 1. Shimadzu atomic absorption spectrophotometer (model no. AA-7000, Kyoto, Japan), which is available at the Ministry of Health and Environment, Baghdad, Iraq, was used to determine the concentrations of the constituents of all water samples in this study.

Fig. 1. Locations of the selected groundwater feedwaters (Mandali, Al-Yusufiya, and Al-Musayyib) in the middle of Iraq.

Two other locations, which are more likely to use groundwater as the feedwater of the RO systems to produce a useable water for different purposes, are Al-Yusufiya location which is one of the southern suburbs of Baghdad and Al-Musayyib location which is located in the north of Babylon province. Two groundwater wells in Al-Yusufiya area were selected to have samples of groundwater and further to analyze them. The analysis of these samples is illustrated in Table 2. Sample 1 which has the highest TDS concentration (2,588 mg/L) was used to represent the feedwater to carry out the RO membrane experiments. However, some difficulties encountered providing samples from the third location which is Al-Musayyib. Therefore, the available analyses of the groundwater quality were used to prepare the feedwater of the conducted RO experiments for this location. A groundwater quality analysis performed by Hill [33] was used to simulate the feed groundwater of Al-Musayyib area. The quality analysis with the highest salinity (3,029 mg/L TDS) was selected to conduct the worse scenario. The measured and the prepared concentrations of the salt ions of this location are shown in Table 3. The salt stock solution was prepared by calculating the required weight of each chemical compound to prepare the measured concentration of the

Table 1
Water analysis of samples 1 and 2 of the groundwater in Mandali location

Parameter	Sample 1	Sample 2
TDS (mg/L)	1,388	1,350
Ca^{+2} (mg/L)	47.8	42.9
Mg^{+2} (mg/L)	23.6	26.94
Na^{+1} (mg/L)	382	428
SO_4^{-2} (mg/L)	806.4	518.4
Cl^{-1} (mg/L)	369.21	175.72

Table 2
The characteristics of feedwaters of Al-Yusufiya

Parameter	Sample 1	Sample 2
TDS (mg/L)	2,588	2,514
Ca^{+2} (mg/L)	226	168
Mg^{+2} (mg/L)	240	75
SO_4^{-2} (mg/L)	2,500	1,070
Cl^{-1} (mg/L)	248	378
NO_3^{-1} (mg/L)	21	26

groundwater quality listed in Table 3. Inorganic salts which are calcium chloride ($CaCl_2.2H_2O$), magnesium sulfate ($MgSO_4.7H_2O$), sodium bicarbonate ($NaHCO_3$), sodium sulfate (Na_2SO_4), calcium chloride ($CaCl_2.2H_2O$), calcium sulfate ($CaSO_4$), magnesium chloride ($MgCl_2.6H_2O$), and calcium nitrate ($Ca(NO_3)_2.4H_2O$) were used to prepare the salt stock solution of Al-Musayyib feedwater. The calculated weight of the salt was added to 500 mL of deionized water. Then, the sample was left on a magnetic stirrer for 24 h to make sure that all the salt is dissolved. After that, the prepared sample was added to a 95.5 L of deionized water to obtain 100 L of water supply. Samples from the prepared stock solution were taken and analyzed by the Shimadzu atomic absorption spectrophotometer to ensure that the concentrations of the prepared solution constituents were close or similar to the selected site water quality.

2.2. Lab-scale RO system

A lab-scale of RO system (manufactured by G.U.N.T. Gerätebau GmbH, Barsbüttel, Hamburg, Germany) which is available at the Environmental Engineering Department, Mustansiriyah University, Baghdad, Iraq, was used in this study. A schematic diagram of the experimental system is shown in Fig. 2. The main part of the RO system is the membrane module which consists of several sheets of TFC PA (FilmTec) RO membrane wrapped around a perforated tube in a spiral shape as shown in Fig. 3. Spiral wound RO membrane module is a cross-flow filtration system which has one influent stream (feed channel) and two effluent streams (permeate and concentrate channels) [9]. The RO membrane is placed inside the high-pressure vessel which has a length of 500 mm and a diameter of 60 mm. The spiral wound RO membrane module is designed to handle a maximum pressure of 1,000 psi (6,895 kPa). The active area of the RO membrane of the used lab-scale is 1.2 m^2. The maximum raw feedwater flow rate of the system is 23 L/min and the maximum operating temperature is 45°C. The system consists of two large tanks; feedwater supply tank (B2) and supply distilled water tank (B3) for rinsing the system. The volume of each tank is 110 L. In addition, the system has a permeate tank (B1) with a volume of 5 L to collect the product water. Several taps in different locations are supplied for draining the system, collecting samples, and manipulating the operation of the system to run the experiments. Also, the system contains pump engine, pulsation damper to protect the pump from cavitation, display and control elements, membrane module (A), measuring cell with conductivity sensor (QI), flow rate sensor (FI), and several valves for multiple purposes such as draining and safety of the system.

Table 3
The characteristics of feedwaters of Al-Musayyib [33]

Parameter	Measured	Prepared
TDS (mg/L)	3,029	2,800–2,950
Ca^{+2} (mg/L)	392	390–394
Mg^{+2} (mg/L)	92.75	88.05–94.5
Na^{+1} (mg/L)	109.94	108–140.9
K^{+1} (mg/L)	18.33	15.5–20.4
SO_4^{-2} (mg/L)	1,167.84	1,164–1,175
Cl^{-1} (mg/L)	194.64	181.6–197
NO_3^{-1} (mg/L)	30.38	30.25–30.5

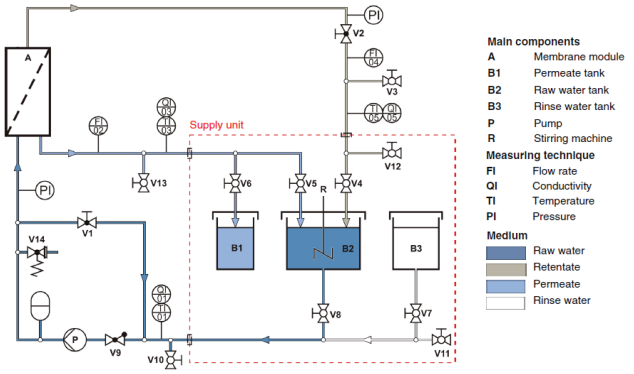

Fig. 2. A schematic diagram of the experimental system [34].

2.3. Autopsy of used RO membrane

A sample of spiral wound RO membrane (aromatic PA composite membrane, model LP21-4040-Vontron membrane technology, USA) after being used for 45 d was brought from an existed pilot RO plant in Mandali for further analysis of the fouling materials deposited on the membrane surface. The membrane was carefully opened and cut to prepare a sample. The sample was sent to the Samuel Roberts Noble Electron Microscopy Laboratory, University of Oklahoma, USA, to image and analyze the sample of the RO membrane. SEM in conjunction with EDXS and secondary ion beam (FIB) was used to examine the materials deposited on the RO membrane surface.

3. Experimental procedures

Before conducting each experiment, the lab-scale RO system was operated by using distilled water as a feedwater to make sure that the system is properly functioning, and no salts ions is existed in the concentrated channel and the permeate carrier by checking the electrical conductivity measurements. After that, a 100 L of feedwater sample was added to the feedwater tank (B2). A stirring machine which is located in the feed tank was operated at a speed of 300 rpm to

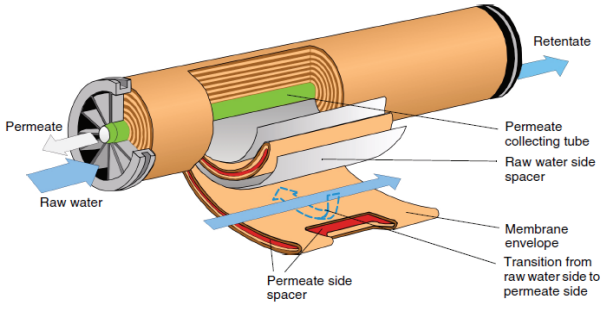

Fig. 3. Spiral wound RO membrane [34].

make sure of the solution homogeneity. Then, the RO system was operated at an applied pressure of 4,000 kPa (40 bar). For the simulated feedwater, a sample from the feedwater tank was taken to have a water analysis at the beginning of each run to ensure that the prepared water quality and the measured water quality are similar or close. Moreover, conductivity, temperature, and pressure for permeate, retentate, and feedwater for all runs were recorded for further analysis and discussion. Furthermore, three samples (at the beginning, middle, and end of each run) were taken from the permeate water to measure the concentration of the ions and hence calculate salt rejection. To avoid exceeding the required applied pressure for each run, the bypass valve (V1) was used to control the system pressure. In addition, each run was conducted with operation time to achieve 70%–75% water recovery of the total volume of the feedwater (100 L). This was performed by recirculating the retentate (brine) into the feedwater tank (B2) and by separately collecting the product (permeate) in the permeate tank (B1) up to the end of each run. The run was stopped when the volume of the collected permeate reached the desired volume (70–75 L). In order to obtain a high feedwater temperature for some runs where the feedwater temperature reaches 40°C, an electrical heater was totally immersed in the feedwater tank (B2). Some of the runs were implemented by using the same RO membrane. In this case, the RO membrane was cleaned with a 0.1% of NaOH solution at the end of the run. Then, the system was rinsed twice with deionized water to make sure that the conductivity of the permeate and the concentrate channels is zero.

4. Results and discussion

Table 4 summarizes the experimental data and results which include run number, location of the feedwater, TDS concentration of feedwater, feedwater pressure, feedwater temperature, permeate flux range of each run, desired water recovery, and total time of each run.

4.1. The performance of the RO system in terms of permeate flux and salt rejection

As previously mentioned, several runs were conducted to investigate the RO membrane system performance in desalting the groundwater of the considered locations. Fig. 4 displays the evolution of the permeate fluxes with the time for Mandali location (run 5 and run 6), Al-Yusufiya location (run 4), and Al-Musayyib location (run 1) whose feedwater was simulated. The RO membrane of run 1 was cleaned with NaOH solution and rinsed with deionized water, then it was used to conduct run 4. The RO system for all runs was operated at an applied pressure of 4,000 kPa (40 bar). Overall, the permeate flux of all runs dropped with the run time. According to previous studies [35,36], the increase of the salt concentration in the feed channel leads to higher fouling layer thickness and higher salt concentration on the membrane surface. The consequence of this process is increased in both permeate flux decline and salt concentration in the permeate channel. Therefore, the drop of the permeate flux is attributed to the accumulation of the materials on the membrane surface which resulted in a reduction in the filtration area [23]. However, in long-term operation system, the permeate flux decreases for a certain time and then becomes more stable [26]. Fig. 4 displays that the initial values of the permeate fluxes for all runs were significantly different. For example, run 1 which was conducted with higher TDS concentration (3,029 mg/L) started at a permeate flux (0.45 Lpm/m^2) while initial permeate flux of run 4 which was conducted with a TDS of 2,588 mg/L was 1.16 Lpm/m^2. In addition run 5, which was carried out with a TDS of 1,388 mg/L, showed the highest permeate flux for all the run time (started at 1.28 Lpm/m^2 and ended at 0.915 Lpm/m^2). Because all runs were implemented under the same conditions, the difference among the permeate fluxes of these runs is likely due to the difference in the groundwater quality. Moreover, the overall permeate flux drop among all runs was also considerably different. Run 6, for instance, had a total permeate flux drop of 36% compared

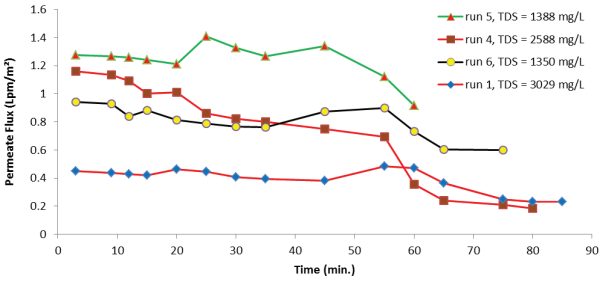

Fig. 4. Permeate flux evolution for Mandali location (run 5 and run 6), Al-Musayyib location (run 1), and Al-Yusufiya location (run 4). The RO system for all runs was operated at an applied pressure of 4,000 kPa (40 bars).

Table 4
Summary of the conducted RO membrane experiments

Run's number	Location	TDS of feedwater (mg/L)	Feed pressure (kPa)	Temperature (°C)	Permeate flux range (Lpm/m²)	Water recovery (%)	Total time (min)
1	Al-Musayyib	3,029	4,000	25	0.45–0.23	75	85
2	Al-Musayyib	3,029	4,000	33	1.83–0.315	75	80
3	Al-Musayyib	3,029	4,000	40	1.77–0.013	70	105
4	Al-Yusufiya	2,588	4,000	25	1.16–0.183	75	80
5	Mandali	1,388	4,000	25	1.28–0.915	75	60
6	Mandali	1,350	4,000	25	0.94–0.6	75	75
7	Al-Musayyib	3,029	5,000	25	1.45–0.631	75	75

with that of run 1 which was 49%. The least total permeate flux drop (28%) was seen in run 5 while the highest total permeate flux drop (84%) was observed in run 4. It is possible to maintain the high value of the initial permeate flux longer by operating the brackish water RO system under appropriate operating conditions and proper conventional pretreatment [26]. Furthermore, the total time to attain the desire water recovery (70% of the total volume of the feedwater) of each run was also varied among the conducted runs. Run 5, for example, had the least run time which was 60 min compared with that of 85 min of run 1. The minimum run time observed in run 5 is attributed to the highest permeate flux and the least total permeate flux drop. The salt rejection rates (in terms of TDS rejection rate) of the conducted runs among the locations were also different as displayed in Fig. 5. Run 2 and run 3 shown in Fig. 5, which represented Al-Musayyib location, were conducted with different feedwater temperatures; therefore, their results were only compared with run 1. Run 5 and run 6 showed high salt rejection rates (98.9% and 98.47%) compared with those of run 1 and run 4 (96.35% and 93.71%). Although the feedwater of run 1 had higher TDS concentration than that of run 4, run 1 exhibited a better performance in salt rejection. The trends of the permeate electrical conductivity curves of runs 1, 4, 5, and 6 which are shown in Fig. 6 consistent with the overall TDS removal efficiency. For example, run 4 showed a significant increase in the permeate conductivity during the run time which resulted in low salt rejection rate (93.71%). Run 5, on the contrary, showed the least values of the permeate conductivity which were slightly increased during the run time. Thus, the salt rejection rate of run 5 (98.9%) was the highest among all operated runs.

In general, run 4 showed more different trends of permeate flux decline and permeate conductivity than those of run 1, run 5, and run 6. This is probably due to using the reactivated RO membrane which was used to conduct run 1. It seems that cleaning with a 0.1% of NaOH solution at the end of the run and, then rinsing the RO system with deionized water was insufficient to totally reactivate the membrane. Using RO membranes in the desalination technology may physically damage them in several ways such as reducing the membrane hydrophobicity, modifying the membrane's texture by changing the pore size and structure, reducing the mechanical strength of the membrane, and reducing the permeability area of the membrane by surface blockage [37]. The dramatic decrease in the permeate flux of run 4 compared with other runs was more likely due to one of the physical damages of the RO membrane. Also, as shown in Fig. 6, the rapid increase in the permeate conductivity of run 4, particularly after 30 min provides additional evidence that the membrane properties were changed during the first run (run 1). Salt ions from the first run that could not be removed by cleaning probably accumulated inside the membrane pores [5,19]. The increase of the salt concentration in the permeate channel is due to the increase in salt ions passage through the membrane which resulted in a lower salt rejection percentage as displayed in Fig. 5.

4.2. The effect of feedwater temperature on permeate flux and salt rejection

As indicated before, Iraq is located in a region where the temperature is extremely varied during the year (ranges from below 0°C during winter to above 55°C during summer). However, Iraq has a very hot climate for most of the year; therefore, feedwater temperatures of 25°C, 33°C, and 40°C were selected. The extreme temperatures may influence the RO system and consequently the performance of the RO membrane. Therefore, the feedwater temperature of the RO system was considered in this study. Using the same prepared groundwater of Al-Musayyib location as the feedwater to run the lab-scale RO system, runs 1, 2, and 3 were performed at the feedwater temperatures of 25°C, 33°C, and 40°C, respectively. The other conditions were the same for all runs. All runs were stopped when the desired water recovery (70%–75%) was achieved. Fig. 7 shows the effect of the feedwater temperature on the permeate flux for the feedwater with TDS range of 2,800–2,950 mg/L. From Fig. 7, it can be seen that the initial permeate flux increased as the temperature of feedwater was raised from 25°C (run 1) to 40°C (run 3). The initial permeate flux for run 1 (0.5 Lpm/m^2) was significantly lower than that of run 2 (1.83 Lpm/m^2) and run 3 (1.775 Lpm/m^2). The permeate flux of run 2, which was carried out at a temperature of 33°C, declined at a high rate from the beginning of the run time to the time of 15 min. After that, it continued to drop but at a slight, constant rate to the time of about 65 min. Then, the permeate flux sharply dropped to the end of the run time where the desired water recovery

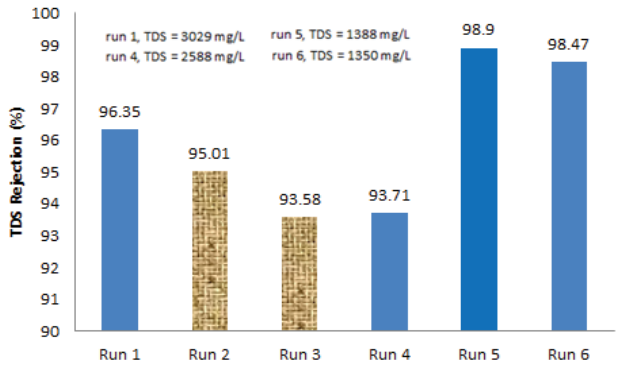

Fig. 5. The salt rejection rate for Mandali location (run 5 and run 6), Al-Musayyib location (run 1, run 2, and run 3), and Al-Yusufiya location (run 4). The RO system for all runs was operated at an applied pressure of 4,000 kPa (40 bars).

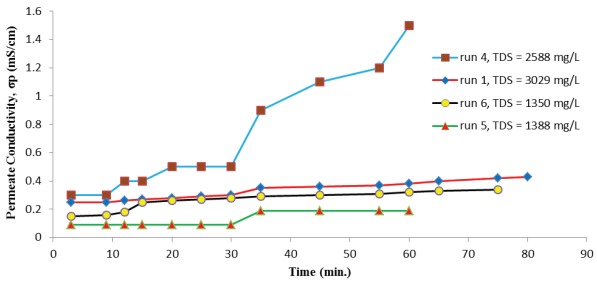

Fig. 6. Permeate electrical conductivity for Mandali location (run 5 and run 6), Al-Musayyib location (run 1), and Al-Yusufiya location (run 4). The RO system for all runs was operated at an applied pressure of 4,000 kPa (40 bars).

was attained. The overall drop of the permeate flux of run 2 was 83% compared with 49% of that of run 1. Although all runs showed a decline in the permeate flux with the time, the trend of the permeate flux for run 3, which was conducted at high temperature (40°C), was quite different. The permeate flux of run 3 increased at the beginning of the run to reach a flux of 2.1 Lpm/m^2 at a time of about 16 min. Then, it was sharply dropped to reach 0.73 Lpm/m^2 at a time of 25 min. After that, it continued to drop at a constant rate to achieve the desired water recovery. The increase in the permeate flux at the beginning of the run can be attributed to the decrease in the water viscosity and the increase in the pore size of the membrane structure [38]. However, increasing the pore size of the membrane likely results in higher salt ions diffusion inside the membrane, which reduced the allowable area of the membrane for the water to pass though [23]. This probably was the reason behind the sudden drop in the permeate flux of run 3. Moreover, higher salt diffusion through the membrane resulted in higher salt ions concentration in the permeate carrier.

The permeate conductivity (σ_p) of the runs conducted at the three different temperatures was recorded and plotted as shown in Fig. 8. The results elucidated that the permeate conductivity of run 1, which was conducted with a temperature of 25°C, started to slightly increase after 5 min of the run time while the permeate conductivity of run 2, which was conducted at a temperature of 33°C, increased after 20 min at a higher rate. However, the permeate conductivity of run 3,

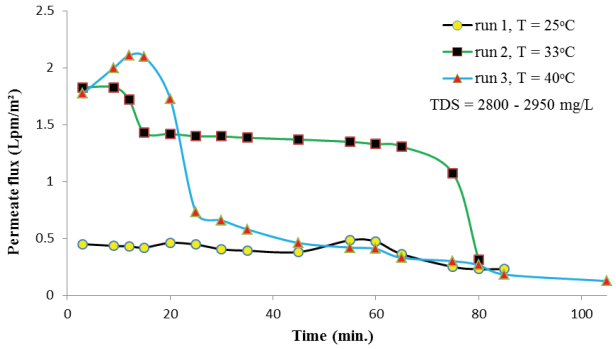

Fig. 7. Effect of feedwater temperature on permeate flux for run 1, run 2, and run 3 (TDS = 2,800–2,950 mg/L).

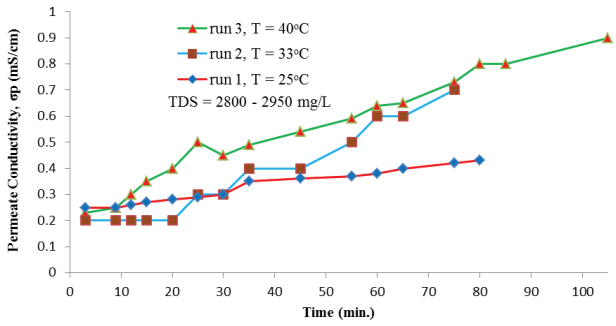

Fig. 8. Effect of feedwater temperatures on permeate electrical conductivity (σ_p) for simulated groundwater samples of Al-Musayyib location (run 1, run 2, and run 3).

which was carried out at 40°C, started to rapidly increase after several minutes of the run time which indicated that more salt ions passed through the membrane and resulted in higher salt concentration in the permeate channel. The overall salt rejection rate of run 1 was 96.35% compared with those of run 2 and run 3 which were, respectively, 95.01% and 93.58% as displayed in Fig. 5. This confirms that the higher temperature of the feedwater allows more solutes to diffuse through the membrane texture and finally to find their way to the permeate carrier. In general, the above results conclude that when the feedwater temperature increases, both the permeate flux and the salt ions passage through the RO membrane increase. This finding is consistent with what was found in the literature [23,39–41].

In order to estimate the salt rejection percentage of the major ions (Na^+, Mg^{+2}, Ca^{+2}, SO_4^{-2}, Cl^-), samples at the beginning (F), middle (M), and end (E) of the run time of each experiment were taken from the permeate tap. Then, analyses to find the concentration of the individual salt ions were conducted. The rejection percentages of the major salt ions for runs 1, 2, and 3, which were conducted at the temperatures of 25°C, 33°C, and 40°C, respectively, are illustrated in Fig. 9. The results demonstrated that the average rejection percentages of the salt ions of run 1 conducted at a lower temperature (25°C) were 85.4%, 94.29%, 97.19%, 94.74%, and 88.94% for Na^+, Mg^{+2}, Ca^{+2}, SO_4^{-2}, and Cl^-, respectively. The average rejection percentages of the salt ions resulted from run 1 are higher than that of the runs (run 2 and run 3) conducted at higher temperatures. For example, the average rejection percentages of the salt ions of run 3 which was carried out at 40°C dropped to 77.5%, 82.68%, 77.95%, 89.9%, and 75.53% for Na^+, Mg^{+2}, Ca^{+2}, SO_4^{-2}, and Cl^-, respectively. Again, the results of the salt rejection percentages confirmed that increasing feedwater temperature enlarged the pore size of the membrane and likely resulted in higher salt ions diffusion inside the membrane and finally higher salt ions concentrations in the permeate carrier.

4.3. The effect of feedwater pressure on permeate flux and salt rejection

In order to investigate the effect of increasing the applied pressure on both permeate flux and salt rejection of the RO membrane, run 7, which its simulated feedwater quality represented the groundwater quality of Al-Musayyib location, was conducted under the same conditions of run 1 except that the feedwater pressure was increased from 4,000 (40 bar) to 5,000 kPa (50 bar). Fig. 10 presents the trends of the permeate fluxes of the two applied pressures for run 1 and run 7. The results showed that a maximum initial permeate flux of 1.452 Lpm/m^2 was obtained at a feed pressure of 5,000 kPa. The overall permeate flux of run 7 which was conducted at a higher feedwater pressure was higher than that of run 1. This confirms that the membrane resistance is pressure dependent [42]. The permeate flux of run 7 declines to about 0.63 Lpm/m^2 with an overall drop of 56.6%. In addition, the total operation time of run 7 was 75 min which was 10 min lower than that of run 1 to achieve the desired water recovery. The shorter time of the run 7 compared with that of run 1 reflects the usual trend found in the literature, that the permeate flux and the feed pressure are proportionally correlated [39,43].

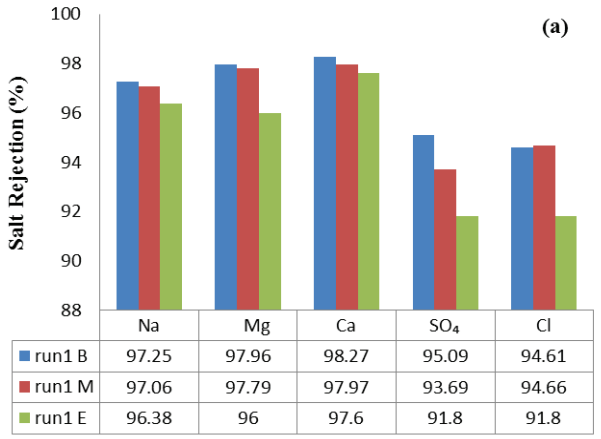

	Na	Mg	Ca	SO_4	Cl
run1 B	97.25	97.96	98.27	95.09	94.61
run1 M	97.06	97.79	97.97	93.69	94.66
run1 E	96.38	96	97.6	91.8	91.8

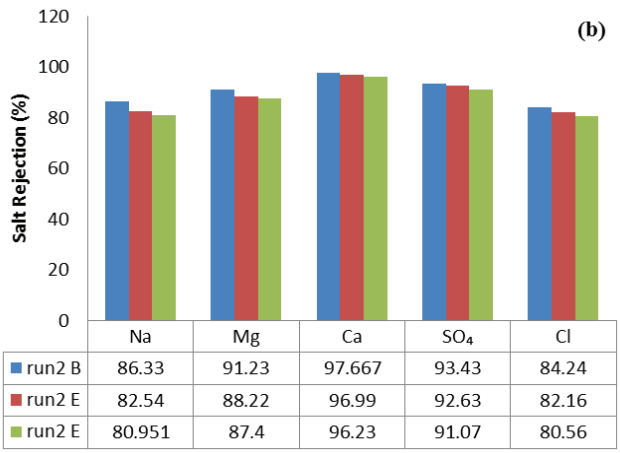

	Na	Mg	Ca	SO_4	Cl
run2 B	86.33	91.23	97.667	93.43	84.24
run2 E	82.54	88.22	96.99	92.63	82.16
run2 E	80.951	87.4	96.23	91.07	80.56

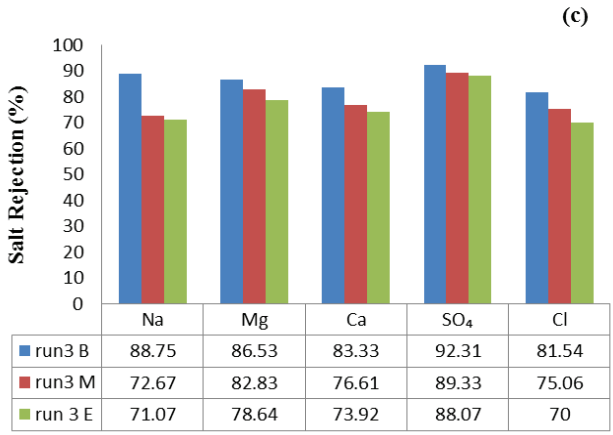

	Na	Mg	Ca	SO_4	Cl
run3 B	88.75	86.53	83.33	92.31	81.54
run3 M	72.67	82.83	76.61	89.33	75.06
run 3 E	71.07	78.64	73.92	88.07	70

Fig. 9. Rejection percentages (R%) of the salt ions of (a) run 1 (T = 25°C), (b) run 2 (T = 33°C), and (c) run 3 (T = 40°C) of the simulated groundwater of Al-Musayyib location (B = begin of the run; M = middle of the run; E = end of the run).

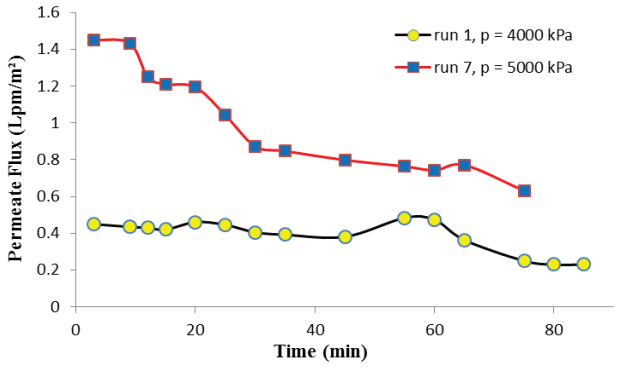

Fig. 10. Effects of feedwater pressure on permeate flux for run 1 and run 7.

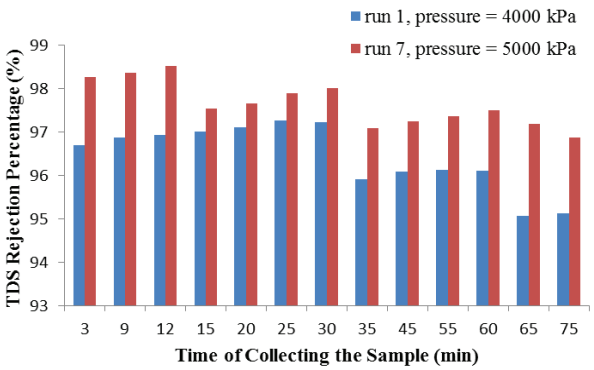

Fig. 11. Effects of feed pressure on salt ions rejection for run 1 and run 7.

Moreover, Fig. 11 shows the effect of the feedwater pressure on the salt rejection rate in terms of TDS concentration in the permeate channel. It can be observed that the percentage of the TDS rejection for run 7, where the feedwater pressure was 5,000 kPa, ranged from 97% to 98% compared with that of run 1, where the feedwater pressure was 4,000 kPa, which ranged from 95% to 97%. In other words, by increasing the applied pressure of the RO system, the quantity and quality of the permeate flux were improved. The improvement of the salt rejection was attributed to the decrease in the salt passage and the increase in the water flux passage through the membrane at higher pressure [9]. This finding was also seen in other studies [40,44] in desalting seawater and brackish water by RO system.

4.4. Foulant analysis by SEM images

SEM images and EDXS spectra were used to examine the materials deposited on the used RO membrane surface. Fig. 12 shows the SEM image (at a magnification of 1,000X) of the scale formation of the materials deposited on the surface of the RO membrane. The morphology of the scale formation apparently covered the entire surface of the RO membrane with a crystal structure. In addition, Fig. 13 shows the SEM image of the same scale formation at a magnification of 7,000X as well as four EDXS spectra in different locations to investigate the predominant elements across the scale formation. The SEM image and the associated EDXS spectra revealed that there was no variation in the scale formation across the membrane surface and the main fouling was inorganic scaling [45]. EDXS spectra analyses exhibited high levels of Ca, C, and O and lower levels of Mg and S. The iridium (Ir) shown in the EDXS spectra is a part of the procedures of the SEM imaging [22]. According to She et al. [45], Tzotzi et al. [46],

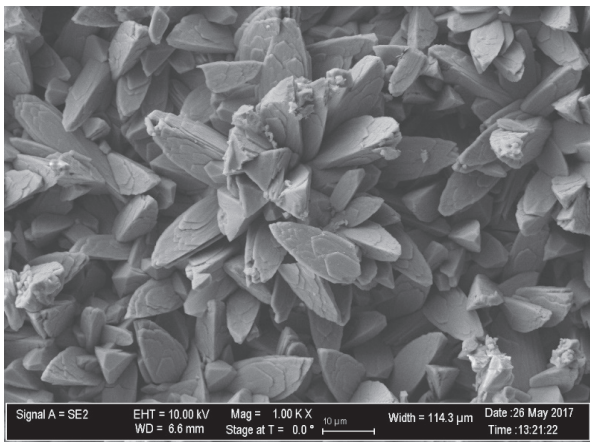

Fig. 12. SEM image of the scale formation of the materials deposited on the surface of the RO membrane for Mandali location.

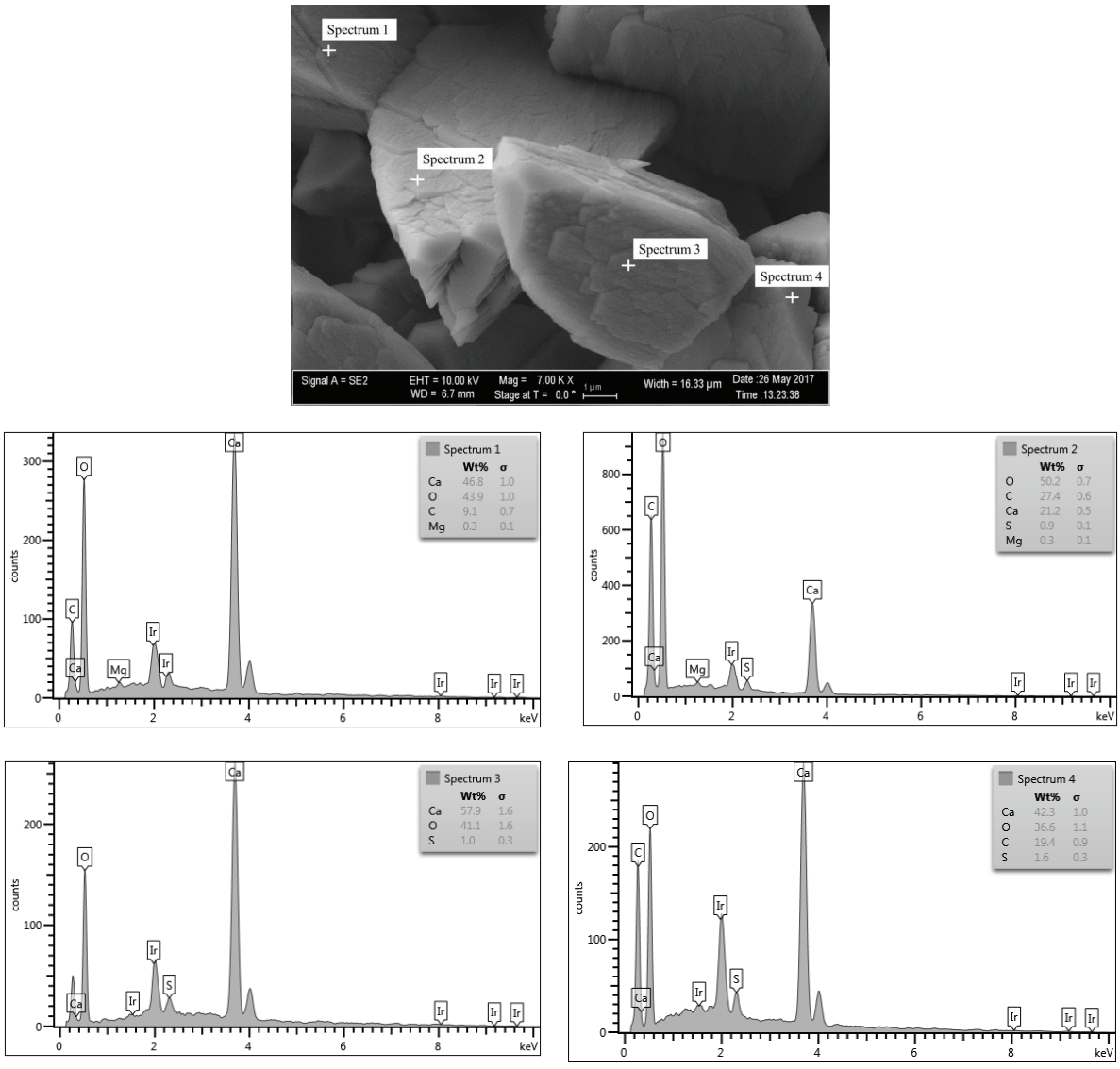

Fig. 13. SEM image at a magnification of 7,000X and the associated EDSX spectra of fouled RO membrane for Mandali location.

and Antony et al. [47], the foulants accumulated on the RO membrane surface is probably calcium carbonate ($CaCO_3$) which was reported as a common scale with all feed types. Moreover, the crystal structure of the deposited material seen in this study is consistent with that observed by [37] is most likely calcite. Antiscalants can be used to inhibit the growth of calcium carbonate scale on the RO membrane surface. A blend of polyacrylic acid and phosphoric acid or polyacrylate and a hydroyethylidene iphosphonate is the most effective antiscalant to control calcium carbonate precipitation. In addition, cleaning chemicals are cautiously used to control calcium carbonate scale. It is mostly recommended that alkaline cleaning is to be conducted first. However, acid cleaning is more appropriate to be conducted first if the calcium carbonate scale is presented on the RO membrane surface [9].

5. Conclusions

The difference in the groundwater quality of the selected locations had a significant impact on the permeate fluxes produced by the RO membrane system. The initial value of the permeate flux of the feedwater with higher TDS concentration (3,029 mg/L) started at a low permeate flux (0.45 Lpm/m^2), while initial permeate flux of feedwater with a lower TDS concentration (2,588 mg/L) started at a high permeate flux 1.16 Lpm/m^2. It is possible to maintain the high value of the initial permeate flux longer by operating the brackish water RO system under appropriate operating conditions and proper conventional pretreatment [26]. In addition, the RO system of Mandali location (run 5 and run 6) which had the least TDS concentration exhibited the highest salt rejection rates (98.9% and 98.47%). Moreover, the feedwater temperature had considerably influenced the permeate flux and the salt rejection of the RO membrane. This was due to the effect of the temperature on the water viscosity and the pore size of the membrane structure. The results of the salt rejection percentages confirmed that increasing feedwater temperature enlarged the pore size of the membrane and likely resulted in higher salt ions diffusion inside the membrane and finally higher salt ions concentrations in the permeate carrier. Because Iraq has a very hot climate for most of the year, it is recommended that the effect of the temperature on the RO membrane performance should be highly considered. Additionally, when the applied pressure of the RO system was increased, both of the permeate flux and the salt rejection of the RO membrane was noticeably improved. Furthermore, foulants analyses by the SEM images and the associated EDXS spectra of the used RO membrane exhibited that the scale formation covered the entire surface of the RO membrane with a crystal structure which was most likely calcium carbonate ($CaCO_3$) and it was apparently in calcite form. Antiscalants can be used to inhibit the growth of calcium carbonate scale on the RO membrane surface. In addition, cleaning chemicals are cautiously used to control calcium carbonate scale [9].

References

[1] P.S. Goh, T. Matsuura, A.F. Ismail, N. Hilal, Recent trends in membranes and membrane processes for desalination, Desalination, 391 (2016) 43–60.

[2] J. Imbrogno, J.J. Keating, J. Kilduff, G. Belfort, Critical aspects of RO desalination: a combination strategy, Desalination, 401 (2017) 68–87.

[3] D.E. Sachit, J.N. Veenstra, Analysis of reverse osmosis membrane performance during desalination of simulated brackish surface waters, J. Membr. Sci., 453 (2014) 136–154.

[4] R.H.S. AL-Suhaili, N.O. Nasser, Water quality indices for Tigris River in Baghdad City, J. Eng., Univ. Baghdad, 14 (2008) 2656–2668.

[5] S. Jiang, Y. Li, B.P. Ladewig, A review of reverse osmosis membrane fouling and control strategies, Sci Total Environ., 595 (2017) 567–583.

[6] G. Foley, Membrane Filtration, A Problem Solving Approach with MATLAB, 1st ed., Cambridge University Press, The Edinburgh Building, Cambridge, UK, 2013.

[7] T.A. Ruehr, E. Ruehr, T.R. Gong, Reverse Osmosis Water Recover Method, Google Patents, Earth Renaissance Technologies, LLC, USA, 2010.

[8] P. Cay-Durgun, C. McCloskey, J. Konecny, A. Khosravi, M.L. Lind, Evaluation of thin film nanocomposite reverse osmosis membranes for long-term brackish water desalination performance, Desalination, 404 (2017) 304–312.

[9] J. Kucera, Reverse Osmosis: Industrial Applications and Processes, 2nd ed., John Wiley & Sons, Inc., Hoboken, New Jersey, 2015.

[10] T.A. Saleh, V.K. Gupta, Membrane Classification and Membrane Operations, Nanomaterial and Polymer Membranes: Synthesis, Characterization, and Applications, Elsevier, Amsterdam, Netherlands, 2016, pp. 55–82.

[11] D.M. Libotean, Modeling the Reverse Osmosis Processes Performance using Artificial Neural Networks, Department of Chemical Engineering, Rovira i Virgili University, Tarragona, Spain, 2007, p. 179.

[12] K.P. Lee, T.C. Arnot, D. Mattia, A review of reverse osmosis membrane materials for desalination—Development to date and future potential, J. Membr. Sci., 370 (2011) 1–22.

[13] I. Koyuncu, R. Sengur, T. Turken, S. Guclu, M.E. Pasaoglu, Advances in Water Treatment by Microfiltration, Ultrafiltration, and Nanofiltration, A. Basile, A. Cassano, N.K. Rastogi, Eds., Advances in Membrane Technologies for Water Treatment: Materials, Woodhead Publishing Series in Energy, Cambridge, UK, 2015, pp. 83–128.

[14] M.L. Davis, Water and Wastewater Engineering: Design Principles and Practice, The McGraw-Hill Companies, Inc., New York, NY, 2010.

[15] A.F. Ismail, M. Padaki, N. Hilal, T. Matsuura, W.J. Lau, Thin film composite membrane—recent development and future potential, Desalination, 356 (2015) 140–148.

[16] N.N. Li, A.G. Fane, W.S.W. Ho, T. Matsuura, Advanced Membrane Technology and Applications, John Wiley & Sons, Inc., Hoboken, New Jersey, 2008.

[17] J. Cotruvo, N. Voutchkov, J. Fawell, P. Payment, D. Cunliffe, S. Lattemann, Desalination Technology: Health and Environmental Impacts, CRC Press Taylor & Francis Group, International Water Association (IWA) Publishing, London, UK, 2010.

[18] National Research Council, Desalination: A National Perspective, The National Academies Press, Washington, D.C., USA, 2008.

[19] L. Malaeb, G.M. Ayoub, Reverse osmosis technology for water treatment: state of the art review, Desalination, 267 (2011) 1–8.

[20] D.E. Sachit, Effect of several parameters on membrane fouling by using mathematical models of reverse osmosis membrane system, Al-Nahrain J. Eng. Sci., 20 (2017) 864–870.

[21] S. Kim, E.M.V. Hoek, Modeling concentration polarization in reverse osmosis processes, Desalination, 186 (2005) 111–128.

[22] D.E. Sachit, J.N. Veenstra, Foulant analysis of three RO membranes used in treating simulated brackish water of the Iraqi marshes, Membranes, 7 (2017) 23.

[23] A. Jawor, E.M.V. Hoek, Effects of feed water temperature on inorganic fouling of brackish water RO membranes, Desalination, 235 (2009) 44–57.

[24] D. Norberg, S. Hong, J. Taylor, Y. Zhao, Surface characterization and performance evaluation of commercial fouling resistant low-pressure RO membranes, Desalination, 202 (2007) 45–52.

[25] T. Tran, B. Bolto, S. Gray, M. Hoang, E. Ostarcevic, An autopsy study of a fouled reverse osmosis membrane element used in a brackish water treatment plant, Water Res., 41 (2007) 3915–3923.
[26] A. Ruiz-García, N. Melián-Martel, V. Mena, Fouling characterization of RO membranes after 11 years of operation in a brackish water desalination plant, Desalination, 430 (2018) 180–185.
[27] H.P. Chu, X.Y. Li, Membrane fouling in a membrane bioreactor (MBR): sludge cake formation and fouling characteristics, Biotechnol. Bioeng., 90 (2005) 323–331.
[28] M. Karime, S. Bouguecha, B. Hamrouni, RO membrane autopsy of Zarzis brackish water desalination plant, Desalination, 220 (2008) 258–266.
[29] H.L. Yang, C. Huang, J.R. Pan, Characteristics of RO foulants in a brackish water desalination plant, Desalination, 220 (2008) 353–358.
[30] W. Arras, N. Ghaffour, A. Hamou, Performance evaluation of BWRO desalination plant—a case study, Desalination, 235 (2009) 170–178.
[31] H.N. Al-Tikrity, Forecasting of Pollution Levels in Accordance with Discharge Reduction in Selected Area on Euphrates River, M.Sc. Thesis, College of Engineering, University of Baghdad, Baghdad, Iraq, 2001.
[32] N. Aghazadeh, A.A. Mogaddam, Assessment of groundwater quality and its suitability for drinking and agricultural uses in the Oshnavieh Area, northwest of Iran, J. Environ. Protect., 1 (2010) 30–40.
[33] S.M. Hill, Qualitative evaluation of the groundwater suitability in Al-Musayyib project area for irrigation, J. Al-Taqani Foundation of Technical Education, 21 (2008) A66–A74.
[34] G.U.N.T., Experiment Instructions; CE530, Reverse Osmosis, G.U.N.T.G. GmbH, Ed., Hamburg, Germany, 2011.
[35] E.M. Hoek, M. Elimelech, Cake-enhanced concentration polarization: a new fouling mechanism for salt-rejecting membranes, Environ. Sci. Technol., 37 (2003) 5581–5588.
[36] A. Alkhudhiri, N. Darwish, N. Hilal, Membrane distillation: a comprehensive review, Desalination, 287 (2012) 2–18.
[37] D.M. Warsinger, J. Swaminathan, E. Guillen-Burrieza, H.A. Arafat, J.H. Lienhard V, Scaling and fouling in membrane distillation for desalination applications: a review, Desalination, 356 (2015) 294–313.
[38] S. Nisan, B. Commerçon, S. Dardour, A new method for the treatment of the reverse osmosis process, with preheating of the feedwater, Desalination, 182 (2005) 483–495.
[39] J.-S. Choi, J.-T. Kim, Modeling of full-scale reverse osmosis desalination system: influence of operational parameters, J. Ind. Eng. Chem., 21 (2015) 261–268.
[40] M. Sarai Atab, A.J. Smallbone, A.P. Roskilly, A hybrid reverse osmosis/adsorption desalination plant for irrigation and drinking water, Desalination, 444 (2018) 44–52.
[41] X. Jin, A, Jawor, S. Kim, E.M.V. Hoek, Effects of feed water temperature on separation performance and organic fouling of brackish water RO membranes, Desalination, 239 (2009) 346–359.
[42] B. Tansel, J. Sager, J. Garland, S. Xu, Effect of transmembrane pressure on overall membrane resistance during cross-flow filtration of solutions with high-ionic content, J. Membr. Sci., 328 (2009) 205–210.
[43] M. Sarai Atab, A.J. Smallbone, A.P. Roskilly, An operational and economic study of a reverse osmosis desalination system for potable water and land irrigation, Desalination, 397 (2016) 174–184.
[44] M. Abou Rayan, I. Khaled, Seawater desalination by reverse osmosis (case study), Desalination, 153 (2003) 245–251.
[45] Q. She, R. Wang, A.G. Fane, C.Y. Tang, Membrane fouling in osmotically driven membrane processes: a review, J. Membr. Sci., 499 (2016) 201–233.
[46] C. Tzotzi, T. Pahiadaki, S.G. Yiantsios, A.J. Karabelas, N. Andritsos, A study of $CaCO_3$ scale formation and inhibition in RO and NF membrane processes, J. Membr. Sci., 296 (2007) 171–184.
[47] A. Antony, J.H. Low, S. Gray, A.E. Childress, P. Le-Clech, G. Leslie, Scale formation and control in high pressure membrane water treatment systems: a review, J. Membr. Sci., 383 (2011) 1–16.